American Journal of Medicine and Medical Sciences 2026, 16(4): 1773-1779
DOI: 10.5923/j.ajmms.20261604.47

Diagnostic and Prognostic Significance of Imaging Modalities in Pediatric Nephroblastoma

Tojiddin Kurbonovich Mustafaev

Candidate of Medical Science, Republican Specialized Scientific and Practical Medical Center of Oncology and Radiology, Ministry of Health of the Republic of Uzbekistan

Abstract **Background:** Nephroblastoma is the most prevalent malignant renal tumor in children, requiring precise diagnostics for accurate prognostication and appropriate therapeutic selection. The efficacy of ultrasound (US), multislice computed tomography (MSCT), and magnetic resonance imaging (MRI) in assessing tumor invasion and the risk of metastasis remains a subject of debate. **Objective:** To evaluate the diagnostic and prognostic utility of US, MSCT, and MRI in pediatric nephroblastoma by correlating radiological data with intraoperative findings. **Materials and Methods:** An analysis was conducted on 90 patients who underwent comprehensive imaging, surgical intervention, and a subsequent 3-year follow-up. Diagnostic efficacy was assessed based on sensitivity, specificity, and predictive values. **Results:** Both US and MRI demonstrated a sensitivity of 87.8%, whereas MSCT exhibited a sensitivity of 84.4%. The specificity for all evaluated modalities was 0%. MRI proved superior in detecting vascular and soft-tissue invasion. Tumor invasion, as identified by MRI and MSCT, was significantly associated with the presence of metastases. **Conclusion:** MRI is the most informative imaging modality for assessing tumor invasion and determining prognosis in pediatric nephroblastoma. A comprehensive approach that incorporates both morphological and intraoperative data is essential.

Keywords Nephroblastoma, Children, Invasion, Imaging, Prognosis

1. Introduction

Nephroblastoma (Wilms tumor) is the most prevalent malignant renal tumor in children, accounting for approximately 6% of all pediatric malignancies and up to 95% of childhood malignant renal neoplasms [2,7]. According to the Surveillance, Epidemiology, and End Results (SEER) data, the annual incidence of nephroblastoma is approximately 8 cases per million children under 15 years of age, with a peak incidence occurring at 3–4 years of age [6] (SEER Cancer Statistics Review, 1975–2020).

The incidence of nephroblastoma varies by ethnicity: it is higher among African American children and lower among Asian populations, highlighting the role of genetic and population-based factors in the etiology of the tumor [4].

The etiopathogenesis of nephroblastoma in the majority of cases is associated with somatic mutations occurring in embryonic renal tissue, frequently involving the *WT1*, *WTX*, and *CTNNB1* genes [8] (Haber D.A., 2005). In a subset of patients, the disease is linked to hereditary syndromes, such as WAGR (Wilms tumor, Aniridia, Genitourinary anomalies, mental Retardation) syndrome, Denys-Drash syndrome, and Beckwith-Wiedemann syndrome, in which the risk of developing nephroblastoma is significantly elevated [5,10].

Received: Mar. 19, 2026; Accepted: Apr. 3, 2026; Published: Apr. 11, 2026
Published online at http://journal.sapub.org/ajmms

These associations indicate that congenital genetic defects play a substantial role in tumor development in a specific patient cohort. According to the International Society of Paediatric Oncology (SIOP), the presence of congenital genitourinary anomalies and other dysplastic changes also elevates the likelihood of nephroblastoma manifestation [15].

Continuing the analysis of the diagnostic aspects of imaging modalities in nephroblastoma, it is essential to emphasize both their strengths and the limitations identified in the present study.

Ultrasound (US) is traditionally utilized as the primary diagnostic modality for pediatric renal tumors. According to Dome et al. (2013), US exhibits high sensitivity in detecting mass lesions, particularly during initial presentation; however, its capability to differentiate vascular and extracapsular invasion is substantially limited [3]. Davidoff (2013) emphasizes that low spatial resolution and significant operator dependence render US an unreliable tool for assessing invasive tumor growth, especially in cases of complex anatomy [2].

Multislice computed tomography (MSCT), as suggested by Shamberger et al. (2001), is more effective in evaluating the anatomical boundaries of the tumor and is particularly indicated for detecting pulmonary metastases, which is crucial for accurate staging [11]. However, as demonstrated in a review by Spreafico et al. (2020), the sensitivity of MSCT in determining vascular invasion remains moderate, and even

with the implementation of contrast-enhanced phases, the accuracy of the method in certain studies does not exceed 70–80% [13].

Conversely, magnetic resonance imaging (MRI), according to Smets et al. (2008), provides superior visualization of soft-tissue structures and vessels, making it the preferred modality when invasion into the inferior vena cava or perinephric fat is suspected [12]. Vujanić et al. (2011) highlight that the sensitivity of MRI in assessing vascular invasion can reach 95%, particularly when specialized sequences are employed [15].

Nevertheless, despite its high sensitivity, as demonstrated in our study, the specificity of all three imaging modalities remains at zero. This is attributed to the absence of reliably confirmed true-negative observations, as well as potential overdiagnosis associated with the clinical caution of the interpreters. According to Spreafico et al. (2020), this phenomenon is typical in pediatric oncology, where even minimal suspicious findings are frequently interpreted as potentially invasive to avoid underestimating the tumor stage [13].

For instance, a study by Varan et al. (2007) demonstrated that signs of extracapsular extension detected by MSCT and MRI are associated with a higher risk of recurrence. The authors emphasize that preoperative evidence of invasion into the vascular bed or adjacent organs can serve as an adverse prognostic marker, especially in bilateral lesions or non-blastomatous components [14].

A study by Chung et al. (2010), based on a cohort of nephroblastoma patients in the USA, also demonstrated that the detection of invasive signs via MRI significantly correlates with an increased rate of metastasis, particularly in cases where the tumor infiltrates the perinephric fat or liver [1].

Concurrently, according to Rogowski et al. (2013), the utility of US in evaluating prognostic features is limited. Despite its widespread availability and safety profile, US is less informative in detecting invasive growth patterns and does not reliably predict the risk of metastasis [9]. The authors note the method's low sensitivity in recognizing vascular invasion and deep tissue penetration, which leads to an underestimation of prognosis in a portion of patients.

Our work also corroborated these observations: the frequency of recurrences and metastases was significantly higher in patients with signs of tumor extension detected by MRI and MSCT, particularly with invasion into the liver, lungs, and inferior vena cava. The differences obtained via MRI reached statistical significance ($p < 0.05$), underscoring the method's potential not merely as a diagnostic tool, but as a prognostic instrument.

Thus, current data indicate that MRI and MSCT possess defined prognostic value in nephroblastoma, particularly in assessing local invasion and its association with the risk of recurrence and metastasis. US, despite its accessibility, remains the method of primary screening but strictly requires confirmation by more accurate modalities when aggressive growth is suspected.

Within the framework of our study, we also aimed to evaluate the prognostic significance of imaging modalities in the context of the risk of recurrence and distant metastasis, taking into account the specific pathways of tumor extension, which formed the basis of the presented analysis.

Objective: To evaluate the diagnostic informativeness of imaging modalities—ultrasound (US), multislice computed tomography (MSCT), and magnetic resonance imaging (MRI)—in determining the direction and characteristics of tumor extension in patients with nephroblastoma. Furthermore, the study aimed to determine their prognostic significance concerning the risk of recurrence and distant metastasis based on correlation with intraoperative and morphological data.

2. Materials and Methods

The study included 90 patients with morphologically verified nephroblastoma who underwent comprehensive treatment and follow-up at the Republican Specialized Scientific and Practical Medical Center of Oncology and Radiology (RSSPMCOR).

Inclusion criteria were: a confirmed diagnosis of nephroblastoma; completion of a comprehensive diagnostic imaging panel, including US, MSCT, and MRI; availability of a detailed surgical protocol describing intraoperative findings; completion of the treatment course including a surgical stage; and a patient follow-up period of at least 3 years post-intervention.

Patients were excluded from the study if they had incomplete imaging data, lacked surgical descriptions or histological verification, experienced a fatal outcome prior to surgical treatment, or had nephroblastoma associated with congenital syndromes where an objective evaluation of independent tumor invasiveness was unfeasible.

Morphological verification was established based on postoperative histological reports, specifying the nephroblastoma variant, extent of spread, and specific features of invasion. Intraoperative data recorded in surgical protocols served as the reference standard for the comparative efficacy assessment of the diagnostic imaging modalities.

Statistical data processing was performed using Pearson's chi-square (χ^2) test to evaluate the significance of differences between groups. The diagnostic efficacy of the imaging modalities was assessed using standard metrics: sensitivity, specificity, accuracy, positive predictive value (PPV), and negative predictive value (NPV). A 2x2 contingency table was utilized as the basis for analysis: true positives (TP), false positives (FP), true negatives (TN), and false negatives (FN).

Calculations were performed using the following formulas:

$$\text{Sensitivity} = TP / (TP + FN),$$
$$\text{Specificity} = TN / (TN + FP),$$
$$\text{Accuracy} = (TP + TN) / (TP + FP + FN + TN),$$
$$\text{PPV} = TP / (TP + FP),$$
$$\text{NPV} = TN / (TN + FN).$$

3. Results

Analysis of the clinical-demographic, morphological, and instrumental characteristics of the patients revealed several patterns reflecting the clinical course of pediatric nephroblastoma managed at a specialized oncological center. The entire cohort (n = 90) received standard therapy, encompassing stages of polychemotherapy, surgical intervention, and, when indicated, radiation therapy, ensuring the completeness of observations and the reliability of the derived conclusions.

The distribution of patients by gender and age is presented in Figure 1. The majority of patients (66.7%) were children under 3 years of age, with a predominance of girls—34 cases (37.8%) compared to 26 boys (28.9%). Among children older than 3 years, there were 17 girls (18.9%) and 13 boys (14.4%), which also reflects a moderate female predominance. Thus, a pronounced accumulation of cases is observed in the younger age cohort, aligning with the well-established epidemiological characteristics of nephroblastoma, which predominantly manifests in early childhood.

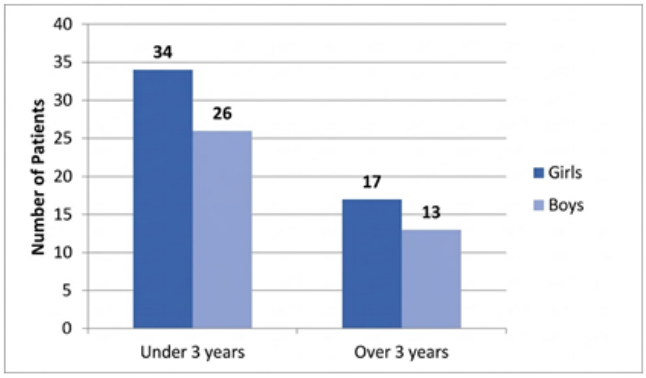

Figure 1. Distribution of patients by gender and age groups

An analysis of the distribution of tumor sizes based on ultrasound (US) data, categorized by the direction of tumor extension, is presented in Table 1. The largest masses (exceeding 15 cm) detected by US were predominantly recorded in cases with invasion into the inferior vena cava, accounting for 25.0% of cases (n=5). Concurrently, another 45.0% of patients with this specific localization had tumors measuring up to 15 cm, indicating pronounced volumetric spread associated with this pattern of extension. In instances of extension into the liver and intestines, tumors generally remained smaller than 15 cm. In patients without signs of invasion, tumors more frequently presented with moderate dimensions: 42.2% measured up to 10 cm, and 39.1% measured up to 15 cm.

Despite the observed differences in the distribution of tumor sizes depending on the direction of extension, the results of the statistical analysis were not significant (χ^2 = 12.13; p = 0.2062). This lack of statistical significance may be attributed both to the limited number of observations in specific subgroups and to the limited sensitivity of US in determining the true dimensions of the tumor in the presence of complex anatomical invasion.

According to the MSCT data presented in Table 2, characteristic differences in tumor size are observed depending on the direction of its extension. In cases of invasion into the inferior vena cava, tumor sizes exceeded 10 cm in the majority of patients: 17.6% had masses larger than 15 cm, and 47.1% had tumors up to 15 cm. A similar pattern is observed with liver invasion, where one-third of the tumors reached over 15 cm. In the absence of extension, tumors more frequently presented with moderate dimensions: up to 10 cm in 48.4% of cases and up to 15 cm in 22.6%.

Interestingly, in the cohort of patients with intestinal invasion, tumors were generally of limited size—66.7% measured up to 10 cm and 33.3% up to 5 cm—which may reflect early diagnosis or the anatomical specificity of this invasion. Despite trends toward differences in tumor size distribution among the groups, statistical significance was not achieved (χ^2 = 18.99; p = 0.0889), likely due to the imbalance in subgroup sizes.

Evaluation of tumor sizes based on MRI data revealed a distinct correlation between the direction of extension and the volume of the lesion (Table 3). In patients with invasion into the inferior vena cava, tumors reached up to 10 cm in the majority of cases (71.4%), and exceeded 15 cm in 14.3%, indicating a high diagnostic sensitivity of MRI for vascular invasion. In the cohort with extension into soft tissues and lungs, tumor sizes were distributed evenly across all intervals, which is likely associated with the heterogeneity of this category and the variability of anatomical spread.

In the absence of signs of invasion, tumors were most often either undetermined or had limited dimensions: in 72.7% of cases, MRI did not visualize extension, and in the remaining cases, sizes did not exceed 15 cm. These data contrast with the larger masses observed in groups with active extension and emphasize the capability of MRI to accurately differentiate tumors with aggressive growth.

Table 1. Distribution of tumor sizes based on US data according to the direction of tumor extension in patients with nephroblastoma (n=90)

Organs (Direction of invasion)	> 15 cm	up to 10 cm	up to 15 cm	up to 5 cm
Intestine	0	1 (100.0%)	0	0
Lungs and soft tissues	5 (25.0%)	5 (25.0%)	9 (45.0%)	1 (5.0%)
Inferior vena cava	0	2 (40.0%)	1 (20.0%)	2 (40.0%)
No extension	6 (9.4%)	27 (42.2%)	25 (39.1%)	6 (9.4%)
χ^2, p	χ^2=12.13, p= 0.2062			

Table 2. Distribution of tumor sizes based on MSCT data according to the direction and characteristics of tumor extension in patients with nephroblastoma

Organs (Direction of invasion)	> 15 cm	up to 10 cm	up to 15 cm	up to 5 cm
Intestine	0	2 (66.7%)	0 (0.0%)	1 (33.3%)
Inferior vena cava	3 (17.6%)	4 (23.5%)	8 (47.1%)	2 (11.8%)
Liver	2 (33.3%)	2 (33.3%)	1 (16.7%)	1 (16.7%)
No extension	8 (12.9%)	30 (48.4%)	14 (22.6%)	10 (16.1%)
No data	0	0	0	2 (100.0%)
χ^2, p	χ^2=18.99, p= 0.0889			

Table 3. Distribution of tumor sizes based on MRI data according to the characteristics of tumor extension in patients with nephroblastoma (n=90)

Organs / Direction of extension	None	> 15 cm	up to 10 cm	up to 15 cm	up to 5 cm
Intestine	0	0	1 (100.0%)	0	0
Lungs and soft tissues	0	1 (25.0%)	1 (25.0%)	1 (25.0%)	1 (25.0%)
Inferior vena cava	0	1 (14.3%)	5 (71.4%)	0	1 (14.3%)
No extension	40 (72.7%)	2 (3.6%)	5 (9.1%)	5 (9.1%)	3 (5.4%)
No data	23 (100%)	0	0	0	0
χ^2, p	χ^2=124.37, p= 0.0000				

Table 4. Association between the direction of tumor extension based on US data and the presence of recurrence and distant metastasis during a 3-year follow-up period in patients with nephroblastoma (n=90)

US Extension Direction	Recurrence		Metastasis		
	Yes	No	Yes	No	No data
Intestine	1 (100.0%)	0	0 (0.0%)	1 (100.0%)	0
Inferior vena cava	0	20 (100.0%)	9 (45.0%)	11 (55.0%)	0
Liver	2 (40.0%)	3 (60.0%)	5 (100.0%)	0	0
No extension	5 (7.8%)	59 (92.2%)	10 (15.6%)	52 (81.2%)	2 (3.1%)
χ^2	18.27		21.94		
p	0.0004		0,0012		

The observed differences were statistically significant (χ^2= 124.37; p < 0.0001), confirming the high informativeness of MRI in assessing the local extent of nephroblastoma.

The association between the direction of tumor extension based on US data and adverse oncological outcomes is presented in Table 4. The presence of invasion into the liver and intestine is characterized by a high recurrence rate: 100% in cases of intestinal invasion and 40% with hepatic involvement. Furthermore, hepatic invasion specifically was associated with a 100.0% rate of distant metastasis, underscoring the highly aggressive nature of this form of local spread. In patients without signs of extension on US, recurrences and metastases were detected significantly less frequently—7.8% and 15.6%, respectively.

In cases of extension into the inferior vena cava, despite its potential anatomical significance, no recurrences were observed; however, distant metastases were diagnosed in almost half of the cases (45.0%), indicating the systemic nature of the neoplastic process.

The observed differences are statistically significant for both the recurrence rate (χ^2 = 18.27; p = 0.0004) and the metastasis rate (χ^2= 21.94; p = 0.0012), which confirms the prognostic significance of assessing the characteristics of tumor extension via US in the examined patients.

In analyzing the prognostic significance of the direction of tumor extension based on MSCT data (Table 5), a distinct association between specific forms of invasion and the risk of distant metastasis is evident. Notably, in patients with hepatic invasion, metastases were detected in 100.0% of cases, unequivocally indicating the highly aggressive nature of this pattern of local spread. Metastatic involvement was also observed in nearly half of the cases with invasion into the inferior vena cava (47.1%), despite the absence of recurrences. This suggests a predominantly systemic nature of tumor dissemination within this cohort.

Intestinal invasion was accompanied by recurrence in one out of three patients, with no distant metastases recorded. In the cohort lacking signs of extension on MSCT, the rates of recurrence and metastasis were substantially lower, at 8.1% and 16.1%, respectively. This underscores the prognostic value of MSCT data in interpreting the tumor growth pattern.

Statistically significant differences were observed regarding the rate of metastasis (χ^2= 26.00$; p = 0.0010), whereas the differences in recurrence rates did not reach statistical significance (χ^2 = 8.55; p = 0.0735), likely due to the limited number of events.

The evaluation of the prognostic significance of MRI data in determining the direction of tumor extension and its

association with adverse outcomes is presented in Table 6. The obtained results demonstrate a pronounced tendency toward an elevated risk of metastasis in the presence of invasion detected by MRI. Specifically, metastases were confirmed in 100.0% of patients with extension into soft tissues and lungs, whereas in cases with invasion into the inferior vena cava, this rate was 42.9%. This confirms the high prognostic sensitivity of MRI, particularly concerning the systemic dissemination of the tumor.

In the cohort lacking signs of extension on MRI, the rates of recurrence and metastasis were substantially lower, at 5.4% and 16.4%, respectively. The "no data" category warrants special attention: despite the absence of clear visualization of extension, the metastasis rate in this group was 34.8%. This finding may indicate potential limitations of the modality when evaluating patients with atypical or occult growth patterns.

Table 5. Association between the direction of tumor extension based on MSCT data and the presence of recurrence and distant metastasis during a 3-year follow-up period in patients with nephroblastoma (n=90)

MRI Extension Direction	Recurrence		Metastasis		
	Yes	No	Yes	No	No data
Intestine	1 (33.3%)	2 (66.7%)	0 (0.0%)	3 (100.0%)	0 (0.0%)
Lungs and soft tissues	0 (0.0%)	17 (100.0%)	8 (47.1%)	9 (52.9%)	0 (0.0%)
Inferior vena cava	2 (33.3%)	4 (66.7%)	6 (100.0%)	0 (0.0%)	0 (0.0%)
No extension	5 (8.1%)	57 (91.9%)	10 (16.1%)	50 (80.6%)	2 (3.2%)
No data	0 (0.0%)	2 (100.0%)	0 (0.0%)	2 (100.0%)	0 (0.0%)
χ^2	8.55		26,00		
p	0.0735		0,0010		

Table 6. Association between the direction of tumor extension based on MRI data and the presence of recurrence and distant metastasis during a 3-year follow-up period in patients with nephroblastoma (n=90)

MRI Extension Direction	Recurrence		Metastasis		
	Yes	No	Yes	No	нет данных
Intestine	0	1 (100.0%)	0	1 (100.0%)	0
Lungs and soft tissues	1 (25.0%)	3 (75.0%)	4 (100.0%)	0	0
Inferior vena cava	0	7 (100.0%)	3 (42.9%)	4 (57.1%)	0
No extension	3 (5.4%)	52 (94.6%)	9 (16.4%)	45 (81.8%)	1 (1.8%)
No data	4 (17.4%)	19 (82.6%)	8 (34.8%)	14 (60.9%)	1 (4.4%)
χ^2	4.92		16.93		
p	0.2960		0,0308		

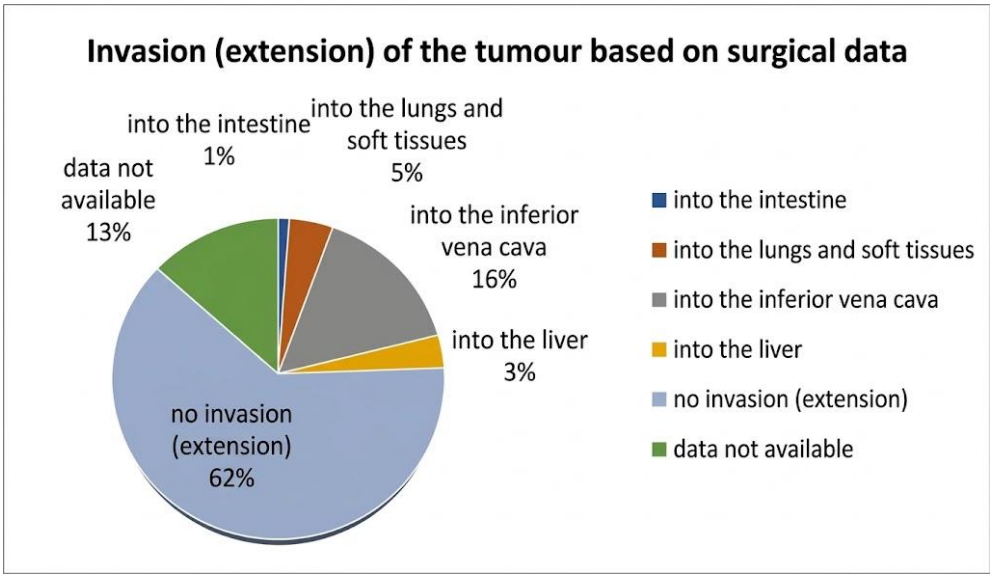

Figure 2. Distribution of tumor extension directions according to the surgical protocol in patients with nephroblastoma (n=90)

Figure 2 illustrates the distribution of the directions of tumor extension based on surgical reports in patients with nephroblastoma. In the majority of cases (62%), tumor extension was not detected intraoperatively, which is likely attributable to predominantly localized growth in certain cases or the effects of neoadjuvant chemotherapy. Among the confirmed forms of invasion, involvement of the inferior vena cava was the most frequently observed (16% of cases), aligning with the characteristic propensity of nephroblastoma for vascular tropism. Invasion into the lungs and soft tissues, as well as the liver, was encountered less frequently (5% and 3%, respectively), while intestinal invasion was noted in only 1% of observations. In 13% of cases, the specific characteristics of tumor extension were not documented in the surgical protocol.

A comparative evaluation of the diagnostic efficacy of three imaging modalities—ultrasound (US), multislice computed tomography (MSCT), and magnetic resonance imaging (MRI)—is presented in Table 7. This analysis is based on a correlation of the imaging findings with the surgical protocol, which served as the reference standard. At first glance, all modalities demonstrate comparably high sensitivity: 87.8% for US and MRI, and 84.4% for MSCT. This indicates the capability of all three techniques to effectively identify cases of tumor extension when present.

However, the specificity of each modality was found to be 0%, indicating an inability to reliably exclude extension in its absence. In other words, all modalities are prone to overdiagnosis, identifying signs of invasion even in cases where it was not surgically confirmed. This effect may be attributed to both the anatomical limitations of imaging and the interpretation of data in the presence of ambiguous findings.

Diagnostic accuracy, as an aggregate metric, was highest for US and MRI (75.6% each) and slightly lower for MSCT (68.9%). The positive predictive value (PPV) mirrors the sensitivity values due to the zero specificity. The negative predictive value (NPV) was also zero across all modalities, stemming from the absence of true negative cases in this cohort.

Thus, despite high sensitivity, all three modalities possess limited prognostic reliability regarding the exclusion of invasion. This underscores the necessity for multidisciplinary verification of imaging data, particularly during the planning of surgical interventions.

Table 7. Comparative diagnostic efficacy of US, MSCT, and MRI in detecting tumor extension in patients with nephroblastoma compared with the surgical protocol (n = 90)

Metric	US	MSCT	MRI
Sensitivity	87.8%	84.4%	87.8%
Specificity	0.0%	0.0%	0.0%
Accuracy	75.6%	68.9%	75.6%
Positive Predictive Value (PPV)	87.8%	84.4%	87.8%
Negative Predictive Value (NPV)	0.0%	0.0%	0.0%

4. Discussion

The findings of this study reflect the clinicomorphological characteristics of nephroblastoma in pediatric patients who underwent comprehensive multimodal treatment. The observed predominance of cases in children under 3 years of age and the female preponderance align with the well-established global epidemiology of the disease [2].

According to US data, the largest tumor dimensions were recorded in cases involving inferior vena cava infiltration; however, these differences did not reach statistical significance. Similar trends in tumor size assessment via MSCT are corroborated by the work of Vorobyov et al. (2017), which noted a relative advantage of MSCT in evaluating tumor volume, though not specifically in stratifying the degree of invasiveness.

Our findings are consistent with the conclusions of Smith et al. (2015), who reported that MRI is superior to other imaging modalities in identifying soft-tissue and vascular invasion in pediatric renal tumors. Their results, obtained in a cohort of 72 children, demonstrated a sensitivity of 90% for this modality.

The zero specificity observed for US, MSCT, and MRI in the current study may be attributed to the absence of true-negative cases within the cohort, as well as the diagnostic tendency toward overdiagnosis even when only minimal signs of invasion are present. These results align with the broader concept of early imaging as a critical component of surgical planning for renal malignancies [Vujanic et al., 2011; 13].

5. Conclusions

The conducted analysis demonstrated that despite the high sensitivity of all three imaging modalities—US, MSCT, and MRI—in detecting the invasive growth of nephroblastoma, none possess sufficient specificity to reliably exclude extension. MRI demonstrated the highest prognostic informativeness regarding the assessment of vascular and soft-tissue invasion, particularly in cases involving the inferior vena cava and extrarenal structures.

Nevertheless, the instances of overdiagnosis highlight the necessity of mandatory correlation of imaging data with the clinicomorphological profile and intraoperative findings. The findings underscore the importance of a comprehensive approach to nephroblastoma diagnostics and confirm that the evaluation of tumor extension must rely on a combination of imaging data and intraoperative verification when formulating surgical and therapeutic strategies.

REFERENCES

[1] Chung E.M., Graeber A.R., Conran R.M. Wilms Tumor:

Modern Imaging and Clinical Perspective. Radiographics. 2010; 30(5): 1257–1271.

[2] Davidoff A.M., Giel D.W., Jones D.P. et al. The feasibility and outcome of nephron-sparing surgery for children with bilateral Wilms tumor: a report from the Children's Oncology Group. Cancer. 2009; 115(18): 4258–4266.

[3] Dome J.S., Fernandez C.V., Mullen E.A., et al. Children's Oncology Group's 2013 blueprint for research: renal tumors. Pediatr Blood Cancer. 2013; 60(6): 994–1000.

[4] Green D.M., Breslow N.E., Beckwith J.B., et al. Effect of age at diagnosis on the prognosis of patients with Wilms' tumor. J Clin Oncol. 2019; 37(6): 531–540.

[5] Grundy P.E., Breslow N.E., Li S., et al. Prognostic factors for children with recurrent Wilms' tumor: results from the Second and Third National Wilms' Tumor Study. J Clin Oncol. 2005; 23(29): 7312–7321.

[6] Howlader N., Noone A.M., Krapcho M., et al. SEER Cancer Statistics Review, 1975–2020. National Cancer Institute. https://seer.cancer.gov.

[7] National Cancer Institute. Childhood Wilms Tumor Treatment (PDQ®)–Health Professional Version. Updated July 2023.

[8] Rivera M.N., Haber D.A. Wilms' tumour: connecting tumorigenesis and organ development in the kidney. Nat Rev Cancer. 2005; 5(9): 699–712.

[9] Rogowski W., Vujanić G.M., Stoneham S.J., et al. Imaging-based risk stratification in Wilms tumour: are we there yet? Eur J Cancer. 2013; 49(14): 3063–3067.

[10] Scott R.H., Stiller C.A., Walker L., Rahman N. Syndromes and constitutional chromosomal abnormalities associated with Wilms tumour. J Med Genet. 2006; 43(9): 705–715.

[11] Shamberger R.C., Ritchey M.L., Haase G.M., et al. Surgical complications after nephrectomy for Wilms' tumor: report from the National Wilms Tumor Study Group. J Am Coll Surg. 2001; 192(1): 63–68.

[12] Smets A.M., van Rijn R.R., Stoker J., et al. Imaging children with Wilms tumor: results of a SIOP imaging survey. Pediatr Blood Cancer. 2008; 50(2): 247–250.

[13] Spreafico F., Bellani F.F., Terenziani M. Wilms tumor: current therapeutic issues and future perspectives. Pediatr Hematol Oncol. 2020; 37(6): 463–476.

[14] Varan A., Akyüz C., Kutluk T., et al. Prognostic significance of radiological findings in Wilms tumor. Pediatr Hematol Oncol. 2007; 24(5): 373–380.

[15] Vujanić G.M., Sandstedt B., Harms D., et al. Revised International Society of Paediatric Oncology (SIOP) working classification of renal tumors of childhood. Med Pediatr Oncol. 2002; 38(2): 79–82.